
Article:
Yu, H, Ingram, N orcid.org/0000-0001-5274-8502, Rowley, JV orcid.org/0000-0001-6646-1676 et al. (2 more authors) (2020) Meticulous Doxorubicin Release from pH-responsive Nanoparticles Entrapped within an Injectable Thermoresponsive Depot. Chemistry – A European Journal, 26 (59). pp. 13352-13358. ISSN 0947-6539

https://doi.org/10.1002/chem.202000389

Meticulous Doxorubicin Release from pH-Responsive Nanoparticles Entrapped within an Injectable Thermoresponsive Depot.

*Huayang Yu, Nicola Ingram, Jason V. Rowley, David C. Green and Paul D. Thornton**

H. Yu, J. V. Rowley, Dr D. C. Green, Dr P. D Thornton

School of Chemistry, University of Leeds, Leeds, LS2 9JT, United Kingdom.

*p.d.thornton@leeds.ac.uk

Dr N. Ingram

Leeds Institute of Biomedical and Clinical Sciences, Wellcome Trust Brenner Building, St James's University Hospital, Leeds, LS9 7TF, United Kingdom.

Keywords: Drug delivery; pH-responsive polymers; thermoresponsive polymers; injectable gels; poly(amino acids); RAFT polymerisation.

Abstract

The dual stimuli-controlled release of doxorubicin from gel-embedded nanoparticles is reported. Non-cytotoxic polymer nanoparticles are formed from poly(ethylene glycol)-*b*-poly(benzyl glutamate) that, uniquely, contain a central ester link. This connection renders the nanoparticles pH-responsive, enabling extensive doxorubicin release in acidic solutions (pH 6.5), but not in solutions of physiological pH (pH 7.4). Doxorubicin-loaded nanoparticles were found to be stable for at least 31 days and lethal against the three breast cancer cell lines tested. Furthermore, doxorubicin-loaded nanoparticles could be incorporated within a thermoresponsive poly(2-hydroxypropyl methacrylate) gel depot, which forms immediately upon injection of poly(2-hydroxypropyl methacrylate) in dimethyl sulfoxide solution into aqueous solution. The combination of the poly(2-hydroxypropyl methacrylate) gel and poly(ethylene glycol)-*b*-poly(benzyl glutamate) nanoparticles yields an injectable doxorubicin delivery system that facilities near-complete drug release when maintained at elevated temperatures (37 °C) in acidic solution (pH 6.5). In contrast, negligible payload release occurs when the material is stored at room temperature in non-acidic solution (pH 7.4). The system has great potential as a vehicle for the prolonged, site-specific, release of chemotherapeutics.

1. Introduction

The design of effective methods to deliver anti-cancer drugs in a controlled manner is a key goal of medicinal chemistry.[1] Materials which assist with drug encapsulation and distribution must prolong the circulation lifetime of drug molecules, and reduce the toxicity of free chemotherapeutic molecules on healthy cells.[2] The development of innovative systems that can encapsulate appreciable drug concentrations, before releasing the drug at a targeted, or localised, site is essential for precise cancer treatment in the absence of side-effects.

Polymeric nanoparticles are promising materials for drug delivery vehicles owing to their capability to encapsulate and distribute poorly water-soluble therapeutic molecules *in vivo*.[3] Polymers can also be designed to have sensitivity to a variety of stimuli; changes in environmental temperature[4] and pH,[5] the presence of a particular enzyme,[6] light irradiation,[7] and the presence of a magnetic field can trigger payload release from polymeric particles.[8] Altered environmental pH is particularly relevant as an actuator for chemotherapeutic release as cancerous tissue (pH 5-pH 6.8) is more acidic than both healthy tissue and the blood (pH 7.4).[9] However, many nanoparticles proposed as potential drug delivery vehicles lack biodegradability *in vivo*, and long-term stability whilst stored prior to administration, rendering their practical application unworkable. Consequently, there is an urgent demand for polymer nanoparticles that preserve drug molecules within their structure for prolonged periods prior to administration, before releasing the therapeutic payload at a controlled rate at a target site upon injection (*in vivo*).

Poly(α-amino acid)s (PAAs) are excellent candidates to be deployed as drug delivery vehicles. owing to their capability to readily self-assemble into discrete, stable, structures in solution.[10] In addition, PAAs are bio-derived, present a wide-range of functional groups, and offer biodegradability and biocompatibility.[11] Ring-opening polymerisation (ROP) of α-amino acid N-carboxyanhydride (NCA) monomers produces PAAs in an efficient and controlled manner,

enabling the generation of block copolymers that can form materials for controlled release applications.[12] However, there are currently no examples of PAA-based nanoparticles that undergo polymer backbone cleavage and drug release in response to acidic media, such as that presented by tumour tissue, owing to the stability of constituent amide bonds against acid-mediated hydrolysis.

The localised release of chemotherapeutic molecules from polymeric nanoparticles to the tumour site is essential to minimise cytotoxic effects on healthy tissue, and the resultant highly-detrimental physiological side-effects. Polymer-based injectable gels which slowly release the therapeutic to the surrounding, target, tissue, offer an effective method to administer cytotoxic therapeutics *in vivo*.[13] Recently, the creation of a poly(*N*-isopropylacrylamine)-based microgel enriched with the anti-HIV drug Lopinavir has been reported. Solid drug nanoparticles suspended within the *in situ*-forming implant enabled sustained drug release over four months.[14] This acts as an excellent template for the creation nanoparticle-containing depot that forms upon injection into aqueous media, essential for nanoparticle immobilisation at the target site.

In this work, a poly(benzyl-*L*-glutamate)-*b*-PEG (PBLG-*b*-PEG) block copolymer was produced that, crucially, contains an acid-sensitive ester bond between the polymeric blocks. Doxorubicin (Dox)-loaded PBLG-*b*-PEG nanoparticles maintained a stable dispersion with negligible Dox release in aqueous solution of pH 7.4. Conversely, extensive Dox release was observed when the nanoparticles were maintained in acidic solution (pH 6.5). In order to realise an injectable drug delivery system, Dox-loaded nanoparticles were entrapped within a thermoresponsive poly(2-hydroxypropyl methacrylate) (PHPMA) gel depot which prolongs nanoparticle residence time and controls their release at a target site. The combination of PAA-based pH-responsive nanoparticles, and a thermoresponsive gel depot, offers a highly sensitive

injectable delivery system for the meticulously controlled delivery of chemotherapeutic molecules.

2. Results and discussion

2.1 Polymer Synthesis

The hydroxyl group of MeO-PEG was used to initiate the BLG NCA ROP to afford an ester-containing polymer, using MSA as the acid catalyst (**Scheme 1**). The amine group is protonated, restricting propagation, before DIPEA was added to trigger amine deprotonation and polymerisation. PBLG chain lengths of 2, 26 and 35, in PBLG-*b*-PEG_{113}, were synthesised in order to produce nanoparticles of varied dimensions. The chemical structures and molecular weight of PBLG-*b*-PEG macromolecules were confirmed by ^{1}H NMR spectroscopy and APC (**Figures S1-S3 and Table S1**). The extent of PBLG grafting from PEG was determined by normalising the proton environment that corresponds to the four protons of PEG (h in **Figures S1-S3**) and comparing the integration value to peaks that correspond to PBLG (a, b, c, d, i and g in **Figures S1-S3**). This data confirmed the successful preparation of the target block copolymers $PBLG_{2}$-*b*-PEG_{113}, $PBLG_{26}$-*b*-PEG_{113} and $PBLG_{35}$-*b*-PEG_{113}. FTIR analysis was used to confirm the presence of expected ester (1742 cm^{-1}, 1731 cm^{-1}, 1650 cm^{-1} and 1743 cm^{-1}), ether (1096 cm^{-1}), and aromatic groups (745 cm^{-1} and 698 cm^{-1}) (**Figure S4**).

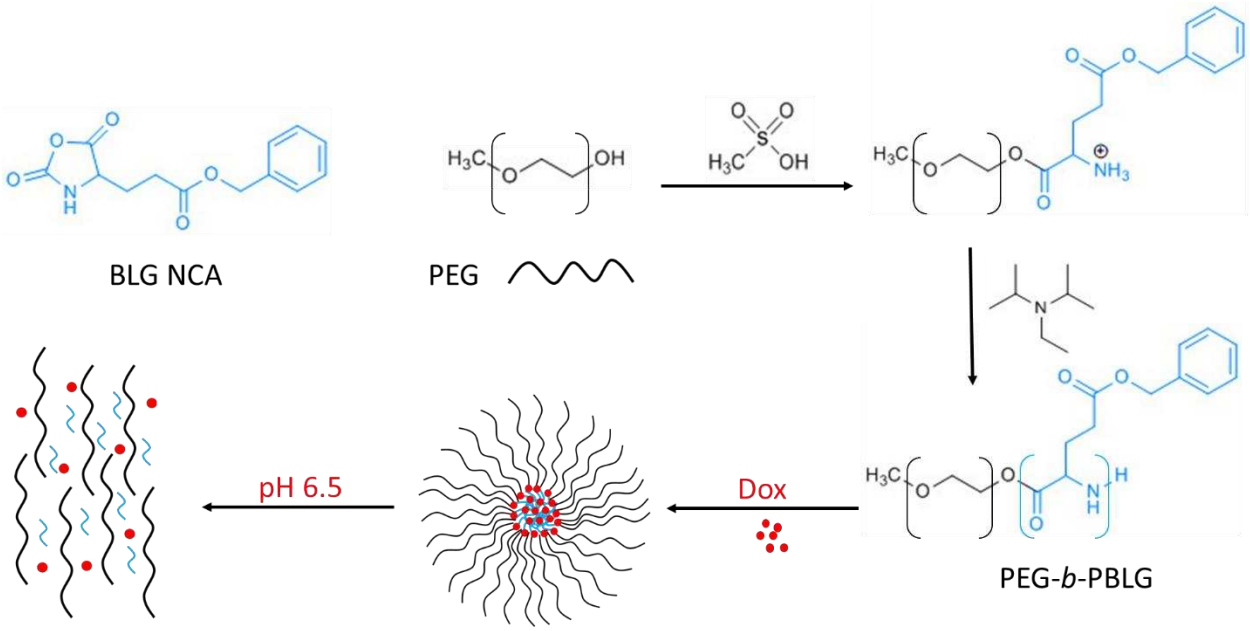

Scheme 1. Reaction outline for the creation of PBLG-*b*-PEG nanoparticles that contain ester linkages to facilitate Dox release when stored in acidic solution.

2.2 Nanoparticle Formation

Nanoparticles were produced from the three polymer types by coacervation.[15] DLS analysis revealed increased nanoparticle size with an increased proportion of hydrophobic PBLG within the block copolymer (**Table 1**). PDI values of $PBLG_2$-*b*-PEG_{113} and $PBLG_{26}$-*b*-PEG_{113} were less than, or close to 0.3, indicating the particle stability. $PBLG_{35}$-*b*-PEG_{113} nanoparticles were considered unstable, after 21 days of storage due to the recorded PDI value (0.437). Therefore, $PBLG_2$-*b*-PEG_{113} and $PBLG_{26}$-*b*-PEG_{113} nanoparticles were chosen for drug release studies due to their appropriate size and PDI values after 21 days storage in aqueous solution. SEM analysis confirmed the presence of spherical nanoparticles (**Figure S5**).

Table 1. DLS data of $PBLG_2$-*b*-PEG_{113}, $PBLG_{26}$-*b*-PEG_{113} and $PBLG_{35}$-*b*-PEG_{113} nanoparticles after 21 days. The hydrophobic content refers to the number of PBLG repeat units as a percentage of the total polymer repeat units.

Copolymers	Hydrophobic chain length (%)	Size (nm)	PDI
$PBLG_2$-*b*-PEG_{113}	1.7	85 ±9	0.284
$PBLG_{26}$-*b*-PEG_{113}	18.7	158 ±2	0.327
$PBLG_{35}$-*b*-PEG_{113}	23.6	311 ±3	0.437

The dimensions of Dox-loaded $PBLG_2$-*b*-PEG_{113} and $PBLG_{26}$-*b*-PEG_{113} nanoparticles were then measured by DLS (**Table 2**). In both cases the mean nanoparticle diameter was less than 200 nm. The PDI values corresponding to $PBLG_2$-*b*-PEG_{113} exceeded 0.3, but the PDI values corresponding to $PBLG_{26}$-*b*-PEG_{113} nanoparticles remained less than 0.3, even after 21 days storage in solution.

Table 2. DLS data revealing the size and stability of Dox-loaded $PBLG_2$-*b*-PEG_{113} and $PBLG_{26}$-*b*-PEG_{113} nanoparticles in water.

Copolymers	24 h		7 days		14 days		21 days	
	Size (nm)	PDI	Size (nm)	PDI	Size (nm)	PDI	Size (nm)	PDI
$PBLG_2$-*b*-PEG_{113}	94 ±5	0.478	93 ±4	0.681	91 ±7	0.533	86 ±8	0.618
$PBLG_{26}$-*b*-PEG_{113}	160 ±11	0.234	162±16	0.225	160 ±18	0.231	161 ±19	0.233

2.3 Dox Release Studies

Dox release studies from $PBLG_2$-*b*-PEG_{113} and $PBLG_{26}$-*b*-PEG_{113} nanoparticles were performed in both pH 7.4 (PBS) and pH 6.5 (TRIS acetate) buffer solutions. Extremely limited loading efficiencies of 4.95% (loading per total polymer mass) were recorded for Dox

encapsulation within $PBLG_2$-*b*-PEG_{113} nanoparticles in both pH 6.5 and pH 7.4 aqueous solution. In contrast, Dox loading efficiencies of 43.9% were recorded for $PBLG_{26}$-*b*-PEG_{113} nanoparticles in solutions of pH 6.5 and pH 7.4. Such enhanced drug loading may be ascribed to the more sizeable hydrophobic compartment that $PBLG_{26}$-*b*-PEG_{113} nanoparticles present. Initially, Dox release was monitored from both nanoparticle sets at 37 °C. After 576 h, Dox release to pH 6.5 solution (38.6%, $PBLG_2$-*b*-PEG_{113}. 23.8%, $PBLG_{26}$-*b*-PEG_{113}) exceeded release to pH 7.4 solution (9.9%, $PBLG_2$-*b*-PEG_{113}. 0.96%, $PBLG_{26}$-*b*-PEG_{113} (**Figure 1**). The rate of release into pH 6.5 buffer solution decreased over time, possibly due to Dox having to travel a greater distance increasingly from the nanoparticle core as time progressed, although release was very gradual; after 48 h Dox release from $PBLG_2$-*b*-PEG_{113} nanoparticles was 10.1% and release from $PBLG_{26}$-*b*-PEG_{113} nanoparticles was 12.1%. The environmental temperature was increased after 576 h to 41 °C as cancer tumour tissue is slightly higher in temperature compared to healthy tissue in the human body,[16] but Dox release was not significantly enhanced. The excessive release of Dox from $PBLG_2$-*b*-PEG_{113} nanoparticles in pH 7.4 solution, coupled with limited Dox loading, rendered the nanoparticles imperfect as potential drug delivery vehicles. However, only 0.96 % of loaded Dox was released from $PBLG_{26}$-*b*-PEG_{113} nanoparticles in pH 7.4 buffer solution after 744 hours; such negligible unwanted release makes this class of nanoparticle an excellent drug delivery vehicle candidate. In a pH 6.5 environment, 24 % of Dox was released progressively from $PBLG_{26}$-*b*-PEG_{113} nanoparticles after 744 hours, offering a system that permits prolonged drug release, minimising the number of repeat administrations that the patient has to suffer.

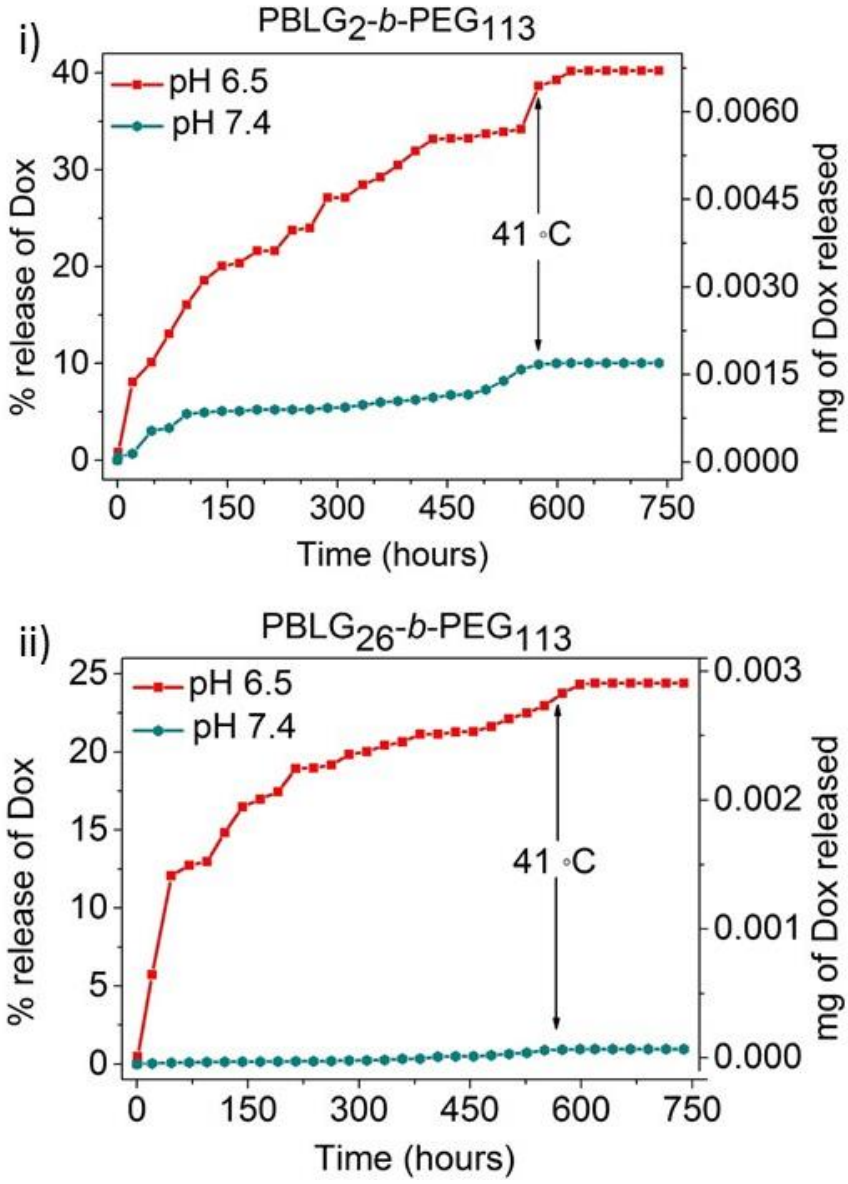

Figure 1. i) Dox release from $PBLG_2$-*b*-PEG_{113} nanoparticles in pH 6.5 and pH 7.4 environments. ii) Dox release from $PBLG_{26}$-*b*-PEG_{113} nanoparticles in pH 6.5 and pH 7.4 environments

2.4 Cytotoxicity Analysis

$PBLG_{26}$-*b*-PEG_{113} nanoparticles that contained, or lacked, Dox were assessed against MCF-7 breast cancer cells, triple-negative breast cancer cells (MDA-MB-231), and Her2-enriched (ER and PR negative) breast cancer cells (MDA-MB-453) in order to assess their ability to treat chemo-refractory disease. Free Dox was used as a positive control (**Table S2**). Negligible cell death was found for empty polymer nanoparticles at 37 °C for all types of breast cancer cells proving $PBLG_{26}$-*b*-PEG_{113} nanoparticles to be non-toxic (**Figure 2**). Dox-loaded nanoparticles were assessed against the same three cancer cell lines, and significant cell death occurred with enhanced polymer concentration. Such nanoparticles were not as lethal as unloaded/free Dox added to the cell types at the same concentration, signifying the effective Dox encapsulation within, and continuous Dox release from, the nanoparticles. The difference in IC_{50} values between the polymer nanoparticles, Dox-loaded nanoparticles, and free Dox are significantly different for each cell line.

The nanoparticles were assessed against non-cancer cell lines to determine if their therapeutic action was specific against cancer cells. HB2 and MCF10A normal breast cell lines were sensitive to Dox delivered *via* nanoparticle encapsulation and as free drug (**Figure S6**). Surprisingly, the polymer nanoparticles demonstrated some cytotoxic effect versus HB2 cells at concentrations of 10 µg/mL and greater, although further studies are required to determine if such extensive nanoparticle accumulation, and cell death, is likely to occur *in vivo.* Although the IC_{50s} values were greater when nanoparticles were employed to encapsulate dox (4.485 µg/mL (nanoparticle) *vs*. 0.201 µg/mL (free dox) for HB2 cells, 10.360 µg/mL (nanoparticle) *vs.* 0.391 µg/mL (free dox) for MCF10A cells), the action of the nanoparticles against non-cancerous cells suggest they are predominantly suited for site specific injection at the tumour site.

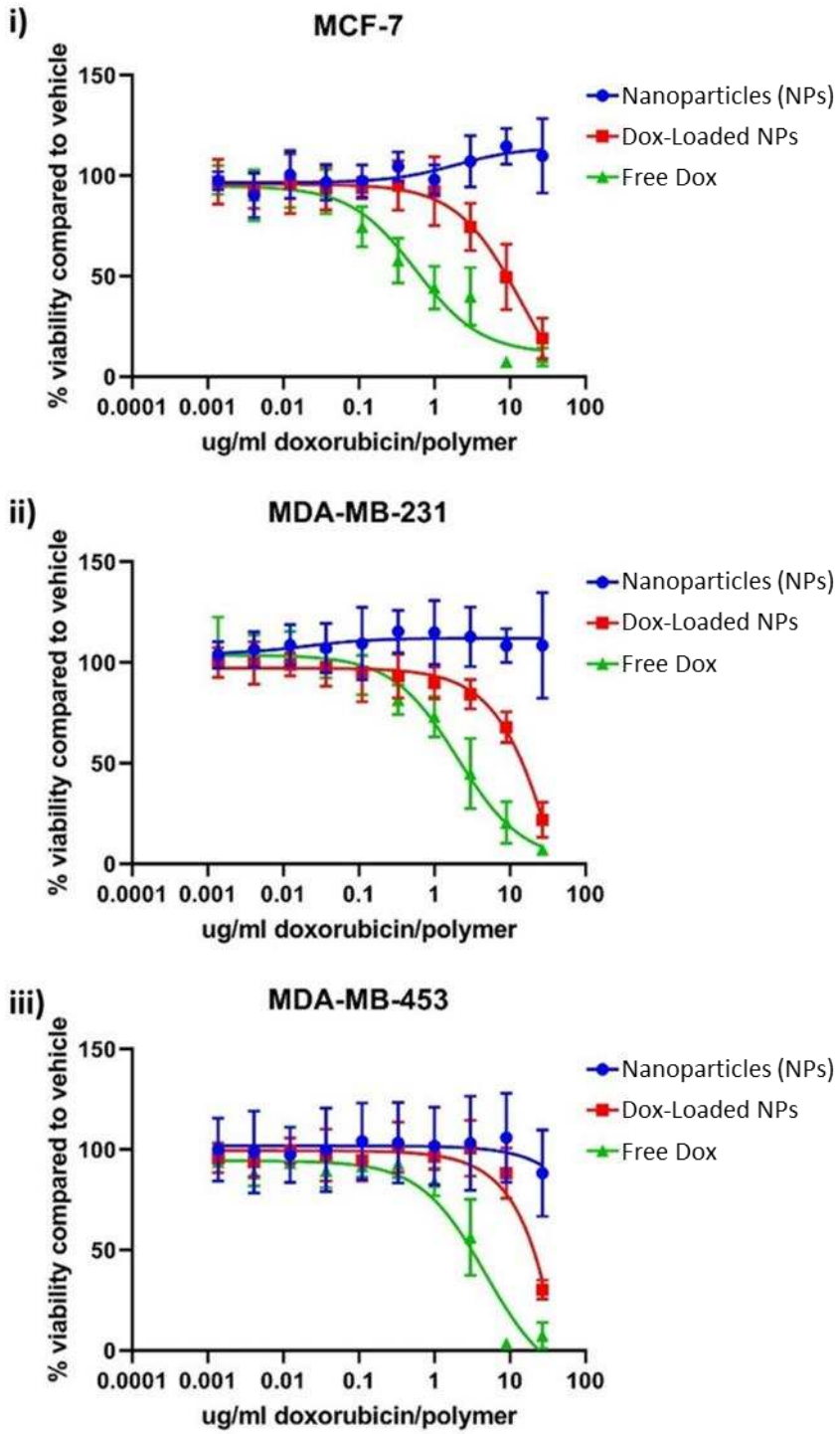

Figure 2. Cytotoxicity of $PBLG_{26}$-*b*-PEG_{113} nanoparticles either empty (NPs) or loaded with Dox (Dox-Loaded NPs), and free Dox on three breast cancer cell lines. Serial dilutions of polymer or Dox-loaded polymer were incubated with i) MCF-7, ii) MDA-MB-231 (triple negative) and iii) MDA-MB-453 (double negative) cell lines.

2.5 $PHPMA_{200}$ Injectable Depot Creation

In order to realise localised Dox release, a polymeric material capable of undergoing a solution to gel transition in aqueous solution was developed. PHPMA was identified as a suitable biocompatible polymer that could act as an injectable vehicle capable of forming a matrix in aqueous solution. Once formed, the matrix holds the nanoparticles specifically at the tumour site, limiting their access to healthy cells. The transformation of PHPMA from solution to gel phase was achieved by dissolving the polymer in DMSO, before injecting the solution into aqueous solution to form a scaffold maintained by polymer chain interactions (**Figure S7**). RAFT polymerisation featuring 4-cyano-4-((phenylcarbonothioyl)thio)pentanoic acid (RAFT agent), AAPH (initiator) and HPMA was performed in an acetone/water mixture, yielding PHPMA with 80 and 200 repeat units. Polymer analysis via ^{1}H NMR spectroscopy, FT-IR spectroscopy and APC (**Figures S8-S10 and Table S4**) confirmed successful PHPMA synthesis. $PHPMA_{80}$ was unable to form stable gels, and therefore could not entrap dox-loaded $PBLG_{26}$-*b*-PEG_{113} nanoparticles, in either pH 6.5 or 7.4 buffered solutions. However, $PHPMA_{200}$ was able to form a depot that contains a vacant core and smooth surface in both aqueous solutions, and so was progressed to be used as the injectable depot (**Figure S11**).

The suitability of $PHPMA_{200}$ as an injectable depot capable of storing Dox-loaded nanoparticles was then determined. Free Dox or Dox-loaded $PBLG_{26}$-*b*-PEG_{113} nanoparticles were added to a $PHPMA_{200}$ solution in DMSO. A depot containing either free Dox or Dox-loaded nanoparticles was then formed by injecting each solution into PBS buffer (**Figure 3**). $PHPMA_{200}$ depot did not sequester free dox, resulting in considerable release of dox into the PBS buffer supernatant (pH 7.4) within 72 hours. Conversely, $PHPMA_{200}$ depot that contained Dox-loaded $PBLG_{26}$-*b*-PEG_{113} nanoparticles withheld the chemotherapeutic payload in PBS buffer (pH 7.4), highlighting the significance of the pH-responsive nanoparticles within the formulation.

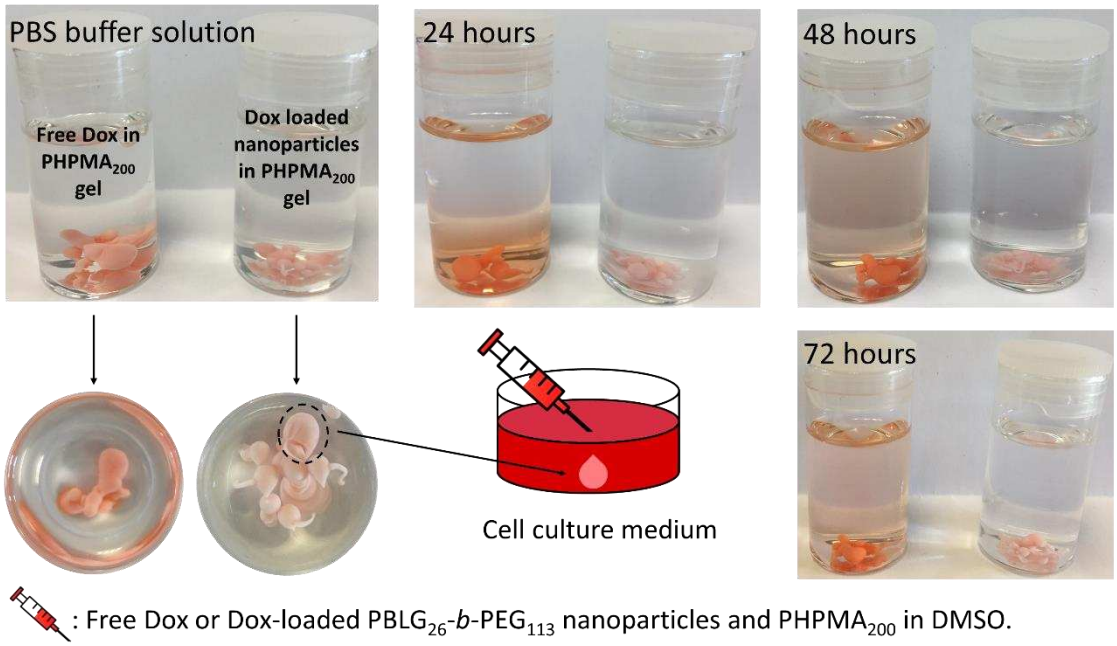

Figure 3. Comparison of free Dox and Dox-loaded $PBLG_{26}$-*b*-PEG_{113} nanoparticles in $PHPMA_{200}$ in PBS buffer solution. Both gels contain an equal mass of Dox; Free Dox loading = 0.063 mg of free Dox, and 0.46 mL of Dox-containing $PBLG_{26}$-*b*-PEG_{113} nanoparticles in DMSO, with 43.9% loading efficiency, contain 0.063 mg of Dox. Details of this calculation are provided in the supporting information.

The cytotoxicity of the $PHPMA_{200}$ depot and $PHPMA_{200}$ depot formed in the presence of Dox-loaded $PBLG_{26}$-*b*-PEG_{113} nanoparticles were determined by injecting PHPMA and Dox-loaded nanoparticles in DMSO, respectively, directly into cell culture medium that contained either MDA-MB-231 triple-negative breast cancer cells or HFFF2 fibroblast cells (**Figure 4**). This was conducted to determine the feasibility of applying the injectable material *in vivo* against normal and cancerous cells. The cell viability of MDA-MB-231 cells remained above 88% after 48 h in all instances; cell viability against the PHPMA depot and the depot with Dox-loaded $PBLG_{26}$-*b*-PEG_{113} nanoparticles incorporated was 88.4% after 48 h. At least 75% of HFFF2 fibroblast cells remained viable after 48 h in all instances; cell viability against the

PHPMA gel with Dox-loaded PBLG$_{26}$-*b*-PEG$_{113}$ nanoparticles included was 85.6% after 48 h. A Two-way ANOVA test was conducted to determine statistical difference between samples/cell lines (**Table S3**). The results demonstrate the appropriateness of the system as an injectable material, particularly for the injection, localisation and potential long-term release of a chemotherapeutic at a tumour tissue site.

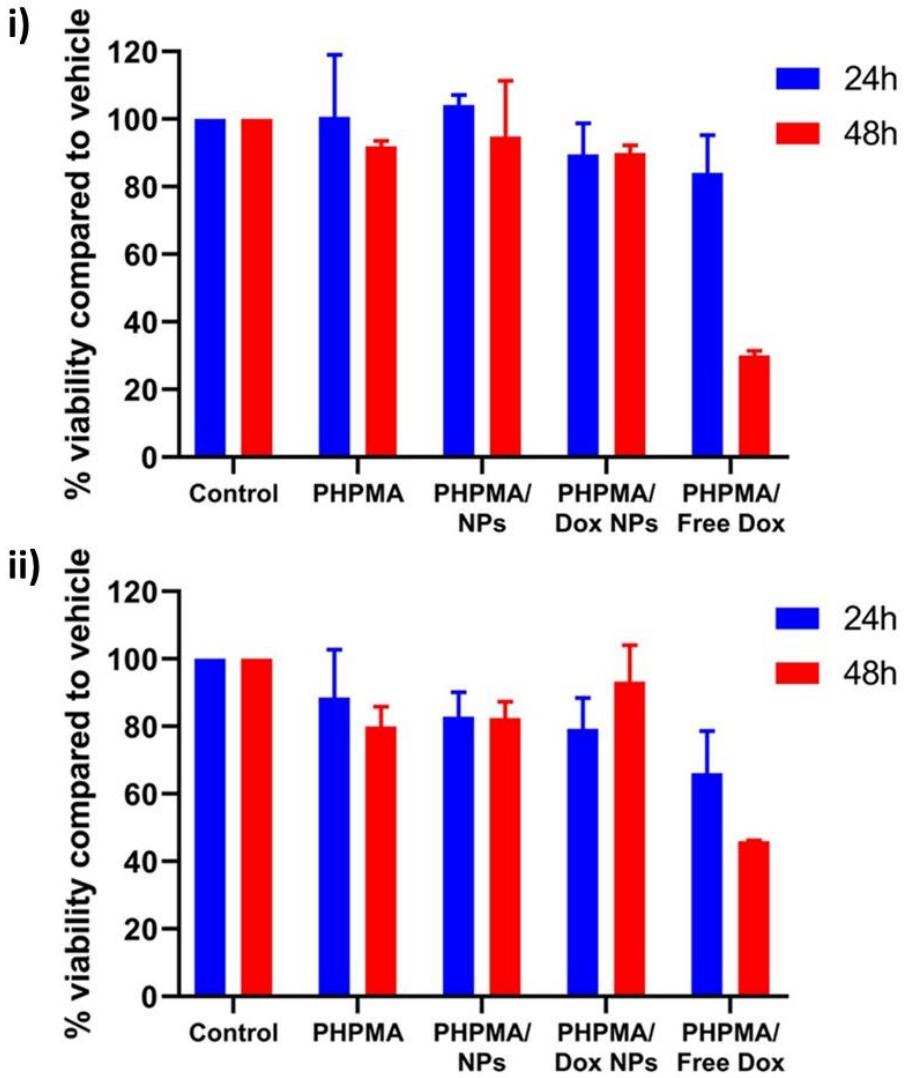

Figure 4. Cell viability studies for the *in situ* formation of PHPMA gel, PHPMA with blank PBLG$_{26}$-*b*-PEG$_{113}$ nanoparticles incorporated, and PHPMA with Dox-loaded PBLG$_{26}$-*b*-PEG$_{113}$ nanoparticles incorporated against i) MDA-MB-231 triple-negative breast cancer cells and ii) HFFF2 fibroblast cells.

2.6 Dox Release from Nanoparticles Embedded within an Injectable $PHPMA_{200}$ Depot

A detailed release study revealed the control over Dox release that the system presents. An insignificant amount of Dox was initially released from $PBLG_{26}$-*b*-PEG_{113} nanoparticles in $PHPMA_{200}$ gel that was maintained in both pH 6.5 acetate buffer solution and PBS buffer solution, either at room temperature or at 37 °C (**Figure 5**). 3.6% Dox release was recorded for the first 192 h when the nanoparticle-loaded gel was maintained in pH 6.5 solution at 37 °C. At this point, enhanced Dox release into the pH 6.5 environment commenced in studies conducted at both room temperature and at 37 °C. After 384 h, 84.2 % of Dox was released from gel stored in pH 6.5 solution at 37 °C. This compares to 40.7% release from gel stored at pH 6.5 at room temperature. Whilst at this time point the depot was intact, it may be surmised that sufficient $PHPMA_{200}$ disassembly had occurred to enable increased interaction between pH 6.5 buffer solution and nanoparticles that have increased mobility, enabling nanoparticle fragmentation and consequent Dox release. When the nanoparticle-loaded gel was maintained in solution of pH 7.4, insignificant Dox release occurred after 500 h, whether the material was heated to 37 °C or not. It can be concluded that Dox release from the reported injectable system is highly sensitive to environmental pH, the extent of release can be modified by changes in external environmental temperature, and that long-term storage (> 500 h) of Dox within nanoparticle encased gels can be realised. The system offers both rapid Dox release (freely-loaded Dox in the $PHPMA_{200}$ depot), and prolonged Dox release from acid-sensitive nanoparticles that are embedded within the injectable $PHPMA_{200}$ depot.

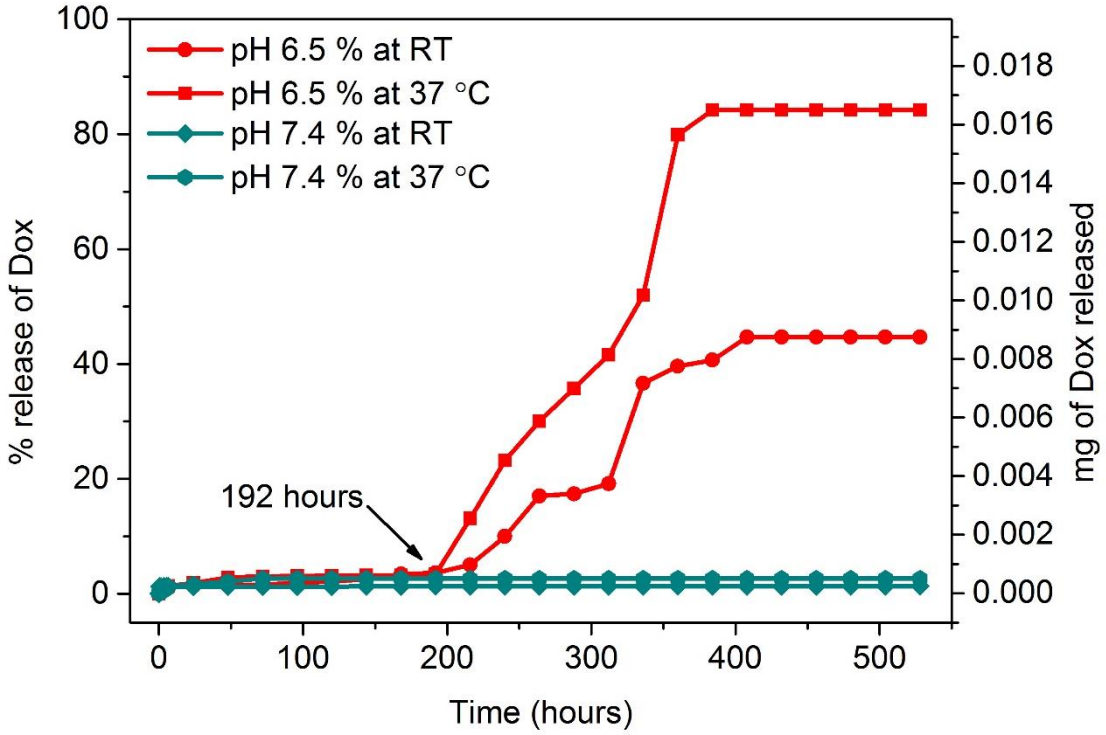

Figure 5. Dox release from PBLG$_{26}$-*b*-PEG$_{113}$ nanoparticles embedded within PHPMA$_{200}$ depot formed in pH 6.5 acetate buffer solution and pH 7.4 PBS buffer solution, at room temperature and at 37 °C.

3. Conclusion

pH-Responsive PBLG-*b*-PEG polymer nanoparticles were synthesised via hydroxyl-initiated NCA ROP. The nanoparticles were well separated and stable in pH 7.4 aqueous environment after 21 days, as revealed by DLS analysis. In a pH 6.5 aqueous environment, a considerable amount of Dox (24 %) was released from PBLG$_{26}$-*b*-PEG$_{113}$ nanoparticles after 31 days due to the intended hydrolysis of the ester links that are an essential feature of nanoparticle design. Crucially, a negligible amount of Dox was released from the nanoparticles when they were maintained in aqueous solution of pH 7.4 after 31 days (0.96 %), suggesting that the formulation may be stored in solution for prolonged periods prior to clinical deployment, an important, but often overlooked, feature of any potential drug delivery system. PBLG$_{26}$-*b*-

PEG_{113} nanoparticles were non-toxic against a variety of breast cancer cell lines, but Dox-loaded $PBLG_{26}$-*b*-PEG_{113} nanoparticles were toxic against the same breast cancer cells. In order to provide a vehicle that enables nanoparticle injection and perpetuation at a cancerous site, a $PHPMA_{200}$ depot was developed that formed upon injection into aqueous solution. A limited amount of Dox was released from Dox-loaded $PBLG_{26}$-*b*-PEG_{113} nanoparticles that were withheld within $PHPMA_{200}$ depot that was maintained within PBS buffer solution, both at room temperature and 37 °C. Dox release was enhanced from the same material when stored in pH 6.5 acetate buffer solution at both room temperature (44.7 %) and 37 °C (84.2%) after 16 days. The combination of pH-responsive $PBLG_{26}$-*b*-PEG_{113} nanoparticles and a thermoresponsive $PHPMA_{200}$ gel depot yields a highly-sensitive injectable delivery system that may be deployed for the localised, highly-controlled and prolonged release of Dox at cancer tumour sites.

4. Experimental Section

4.1 Materials and methods

Methanesulfonic acid (98+ %), *N*-ethyldiisopropylamine (99 %), tetrahydrofuran and TRIS acetate 1.0 M buffer solution pH 6.5 were purchased from Alfa Aesar. Chloroform (99.9 %, extra dry over molecular sieve, stabilised, acroseal) was obtained from ACROS Organics. Triethylamine anhydrous, 4-cyano-4-((phenylcarbonothioyl)thio)pentanoic acid and doxorubicin hydrochloride were obtained from Fluorochem Incorporation. Poly(ethylene glycol)methyl ether (average Mn 5,000), chloroform-d (99.8 atom % D) 2,2'-azobis(2-methyl-propionamidine) dihydrochloride (AAPH), dialysis tubing benzoylated 2000 Da and phosphate buffered saline tablets were obtained from Sigma-Aldrich Corporation. Dimethyl sulfoxide (99.80 % D) was purchased from EURISO-TOP. Diethyl ether (analytical reagent grade) and triethylamine were obtained from Fisher Scientific International Incorporation. Acetone was

purchased from VWR chemicals. BLG NCA and hydroxypropyl methacrylate were obtained from previous PhD students and school of engineering of University of Leeds, respectively.

Nuclear magnetic resonance spectroscopy (NMR, Bruker AVANCE III HD500) and Attenuated total reflection (ATR-PLATINUM) fourier-transform infrared spectroscopy (FTIR, BRUKER ALPHA) were employed to analyse chemical structures, functional groups and chain lengths of the synthesised polymers. Advanced Polymer Chromatography (APC) was used to measure molecular weight of the synthesised polymers. APC was conducted on a Waters Acquity APC system using an Acquity column (Acquity APC TM 200 2.5 μm, 4.5 x 150 mm) and it calibrated against standard poly(methyl methacrylate) samples in tetrahydrofuran (THF). Particle size distribution of each synthesised polymer sample was measured via dynamic light scattering (DLS, Malvern Zetasizer Nano ZSP). Scanning electron microscopy (SEM, FEI NanoSEM 450) was used to analyse size and topography of nanoparticles. Drug release from polymer nanoparticles was measured *via* UV-vis spectroscopy (VARIAN 50 Probe UV-visible Spectrometer).

4.2 Synthesis of PEG-*b*-PBLG

The experiment was conducted as reported by Gradišar *et al.* under a nitrogen atmosphere.[17] Dry chloroform was degassed with nitrogen for one hour. 0.0412 g of BLG NCA, 0.1568 g of poly(ethylene glycol)methyl ether (Meo-PEG) (Mn 5000) and 6.0 μL of methansulfonic acid (MSA) were dissolved in 5.0 mL of dry chloroform. The reaction was stirred in an oil bath at 40 °C for 24 hours. Then the reaction mixture was cooled to room temperature and put in an ice bath. 13 μL of *N*-ethyldiisopropylamine (DIPEA) was added into the reaction mixture. The reaction was stirred at room temperature without nitrogen atmosphere for 24 hours. Then the reaction mixture was added dropwise into cold diethyl ether. Next the solution was centrifuged

for 30 minutes at 4000 rev/ min and dried in a vacuum oven at 45 °C overnight. The product was dialysed against deionised water for 3 days, freeze dried for 2 days then white solids were formed. Different chain lengths of PBLG were prepared which were 2, 26 and 35. The experimental procedures were the same but used different amounts of reactants.

Yield calculation: using molar ratio of reactants and products to calculate theoretical mass of products.

$$\text{Yield} = \frac{\text{Actual mass of product}}{\text{Theoretical mass of product}} \times 100\%$$

4.3 Synthesis of PHPMA

The reaction was in a sealed environment. 0.0297 g of 4-cyano-4-((phenylcarbonothioyl)thio) pentanoic acid was dissolved in 2.0 mL of acetone and 1.0 mL of deionised water. 0.2150 g of AAPH was added in the reaction followed by 1.0 mL of deionised water. When everything dissolved, 3.0521 g of HPMA was added into the reaction followed by 1.0 mL of deionised water. The reaction was stirred at 60 °C overnight and a cream colour gel was formed. Different chain lengths of PHPMA were prepared which were 80 and 200. The experimental procedures were the same but used different amounts of reactants. 0.103 g of $PHPMA_{80}$ and $PHPMA_{200}$ gels were freeze dried, percentages of polymer in each gel were 36.4 % and 65.3 %, respectively.

Supporting Information

Supporting Information is available from the Wiley Online Library or from the author.

References

[1] Y. H. Chao, Y. H. Liang, G. H. Fang, H. B. He, Q. Yao, H. Xu, Y. R. Chen, X. Tang, *Pharmaceutical Research.* **2017**, *34*, 610.

[2] a) W. Cui, J. Li, G. Decher, *Advanced Materials* **2016**, 28, 1302; b) E. Blanco, H. Shen, M. Ferrari, *Nature Biotechnology.* **2015**, *33*, 941; c) V. K. Pawar, Y. Singh, K. Sharma, A. Shrivastav, A. Sharma, A. Singh, J. G. Meher, P. Singh, K. Raval, H. K. Bora, D. Datta, J. Lal, M. K. Chourasia, *Pharmaceutical Research* **2017**, *34*, 1857; d) e) D. Y. Pan, X. L. Zheng, Q. F. Zhang, Z. Q. Li, Z. Y. Duan, W. Zheng, M. Gong, H. Y. Zhu, H. Zhang, Q. Y. Gong, Z. W. Gu, K. Luo, *Advanced Materials* **2020**. doi.org/10.1002/adma.201907490.

[3] a) X. Xu, P. Er Saw, W. Tao, Y. Li X. Ji, S. Bhasin, Y. Liu, D. Ayyash, J. Rasmussen, M. Huo. J, Shi, O. C. Farokhzad, *Advanced Materials* **2017**, 29, 1700141; b) W. C. Li, S. Q. Liu, H. Yao, G. X. Liao, Z. W. Si, X. J. Gong, L. Ren, L. G. Wang, *Journal of Colloid and Interface Science* **2017**, *508*, 145; c) O. S. Fenton, K. N. Olafson, P. S. Pillai, M. J. Mitchell, R. Langer, *Advanced Materials* **2018**, 30, 1705328; d) X. L. Zheng, D. Y. Pan, M. Chen, X. H. Dai, H. Cai, H. Zhang, Q. Y. Gong, Z. W. Gu, K. Luo, *Advanced Materials* **2019**, 31, 1901586.

[4] a) H. Yu, N. Ingram, J. V. Rowley, S. Parkinson, D. C. Green, N. J. Warren, P. D Thornton, *Journal of Materials Chemistry B* **2019**, 7, 7795. b) L. Paasonen, B. Romberg, G. Storm, M. Yliperttula, A. Urtti, W. E. Hennink, *Bioconjugate Chemistry* **2007**, *18*, 2131.

[5] a) W. Zhou, L. Wang, F. Li, W. Zhang, W. Huang, F. Huo, H. Xu, *Advanced Functional Materials* **2017**, 27, 1605465; b) X. Wang, C. Li, N. Fan, J. Li, Z. G. He, J. Sun, *Materials Science & Engineering C-Materials for Biological Applications* **2017**, *78*, 370; c) J. J. Richardson, M. Y. Choy, J. Guo, K. Liang, K. Alt, Y. Ping, J. Cui, L. S. Law, C. E. Hagemeyer, F. Caruso, *Advanced Materials* **2016**, 28, 7703; d) X. Guo, L. Wang, K. Duval, J. Fan, S. Zhou, Z. Chen, *Advanced Materials* **2018**, 30, 1705437; e) C-Y. Sun, Y. Liu, J-Z. Du, Z-T. Cao, C-F. Xu, J. Wang, *Angewandte Chemie International Edition* **2016**, 55, 1010; f) K. Chen, S. S. Liao, S. W. Guo, H. Zhang, H. Cai, Q. Y. Gong, Z. W. Gu, K. Luo, Science China-Materials 2018, 61, 1462.

[6] a) D. Kalafatovic, M. Nobis, J. Y. Son, K. I. Anderson, R. V. Ulijn, *Biomaterials* **2016**, *98*, 192; b) P. D. Thornton, R. J. Mart, R. V. Ulijn, *Advanced Materials* **2007**, 19, 1252; c) Y. Li, G. Liu, X. Wang, J. Hu, S. Liu, *Angewandte Chemie International Edition* **2016**, 55, 1760.

[7] a) Y. Li, J. Sun, Q. P. Chen, Z. P. Chen, L. Zhu, *Nanoscience and Nanotechnology Letters* **2017**, *9*, 982; b) J. Wei, J. Sun, X. Yang, S. Ji, Y. Wei, Z. Li, *Polymer Chemistry* **2020**, 11, 337; c) D. Zhou, J. Guo, G. B. Kim, J. Li, X. Chen, J. Yang, Y. Huang, *Advanced Healthcare Materials*, **2016**, 5, 2493.

[8] a) C. Peters, M. Hoop, S. Pané, B. J. Nelson, C. Hierold, *Advanced Materials* **2016**, 28, 533; b) E. Rafiee, N. Nobakht, L. Behbood, *Research on Chemical Intermediates* **2017**, *43*, 951.

[9] a) M. L. Zhou, M. L. Tang, H. Zhang, K. Luo, Y. Huang, *Journal of Biomedical Nanotechnology* **2019**, *15*, 1688; b) P. Ray, M. Confeld, P. Borowicz, T. Wang, S. Mallik, M. Quadir, *Colloids and Surfaces B-Biointerfaces* **2019**, *174*, 126; c) C. C. Pola, A. R. F. Moraes, E. A. A. Medeiros, R. F. Teofilo, N. F. F. Soares, C. L. Gomes, *Food Chemistry* **2019**, *295*, 671; d) X. J. Chen, T. Y. Niu, Y. Z. Gao, X. Liang, S. N. Li, L. Y. Zhang, L. Li, T. T. Wang, Z. M. Su, C. G. Wang, *Chemical Engineering Journal* **2019**, *371*, 443; e) G. Gao, Y. W. Jiang, W. Sun, Y. X. Guo, H. R. Jia, X. W. Yu, G. Y. Pan, F. G. Wu, *Small* **2019**, *15*.

[10] a) W. Shen, P. He, C. S. Xiao, X. S. Chen, *Advanced Healthcare Materials* **2018**, 7, 1800354; b) M. Khuphe, A. Kazlauciunas, M. Huscroft, P. D. Thornton, *Chemical Communications* **2015**, *51*, 1520; c) C. Grazon, P. Salas-Ambrosio, E. Ibarboure, A. Buol, E. Garanger, M. W. Grinstaff,. S. Lecommandoux, C. Bonduelle, *Angewandte Chemie International Edition* **2020**, 59,622; d) J. H. Jiang, X. Y. Zhang, Z. Fan, J. Z. Du, *ACS Macro Letters* **2019**, *8*, 1216; e) Z. Song, Z. Tan, J. Cheng, *Macromolecules* **2019**, 52, 8521; e) B. S. McAvan, M. Khuphe, P. D. Thornton, *European Polymer Journal* **2017**, 87, 468. f) M. Khuphe, P. D. Thornton, **2018**, Poly(amino acids), 199, *Engineering of Biomaterials for Drug Delivery Systems*, A. Parambath, Elsevier: Amsterdam.

[11] a) X. Zhou, Z, Li, *Advanced Healthcare Materials* **2018**, 7, 1800020;
b) W. H.De Jong, P. J. A. Borm, *International Journal of Nanomedicine* **2008**, 3, 133; T. Borase, A. Heise, *Advanced Materials* **2016**, 28, 5725.

[12] a) M. Khuphe, C. S. Mahon, P. D. Thornton, *Biomaterials Science* **2016**, *4*, 1792; b) Y. Wang, F. Costanza, H. F. Wu, D. Q. Song, J. F. Cai, Q. Li, *Journal of Materials Chemistry B* **2014**, *2*, 3115; c) D. J. Price, M. Khuphe, R. P. W. Davies, J. R. McLaughlan, N. Ingram, P. D. Thornton, *Chemical Communications* **2017**, *53*, 8687; d) J. W. Fan, R. C. Li, H. Wang, X. He, T. P. Nguyen, R. A. Letteri, J. Zou, K. L. Wooley, *Organic & Biomolecular Chemistry* **2017**, *15*, 5145; e) M. Khuphe, N. Ingram, P. D. Thornton, *Nanoscale*, **2018**, *10*, 14201.

[13] a) A. Famili, M. Y. Kahook, D. Park, *Macromolecular Bioscience* **2014**, *14*, 1719; b) J. X. Yan, Y. T. Miao, H. P. Tan, T. L. Zhou, Z. H. Ling, Y. Chen, X. D. Xing, X. H. Hu, *Materials Science & Engineering C-Materials for Biological Applications* **2016**, *63*, 274; c) K. M. Jin, Y. H. Kim, *Journal of Controlled Release* **2008**, *127*, 249.

[14] A. R. Town, M. Giardiello, R. Gurjar, M. Siccardi, M. E. Briggs, R. Akhtar, T. O. McDonald, *Nanoscale* **2017**, *9*, 6302.

[15] M. Khuphe, P. D. Thornton, *Macromolecular Chemistry and Physics* **2018**, *219*.

[16] a) X. J. Zhang, S. W. Niu, G. R. Williams, J. R. Wu, X. Chen, H. Zheng, L. M. Zhu, *Carbohydrate Polymers* **2019**, 221, 84; b) Z. Ferjaoui, E. J. Al Dine, A. Kulmukhamedova, L. Bezdetnaya, C. S. Chan, R. Schneider, F. Mutelet, D. Mertz, S. Begin-Colin, F. Quiles, E. Gaffet, H. Alem, *ACS Applied Materials & Interfaces* **2019**, 11, 30610; c) D. Atanackovic, K. Pollok, C. Faltz, I. Boeters, R. Jung, A. Nierhaus, K. M. Braumann, D. K. Hossfeld, S.

Hegewisch-Becker, *American Journal of Physiology-Regulatory Integrative and Comparative Physiology* **2006**, 290, R585.

[17] Š. Gradišar, E. Žagar, D. Pahovnik, *ACS Macro Letters* **2017**, 6, 637.

Scheme 1. Reaction outline for the creation of PBLG-*b*-PEG nanoparticles that contain ester linkages to facilitate Dox release when stored in acidic solution.

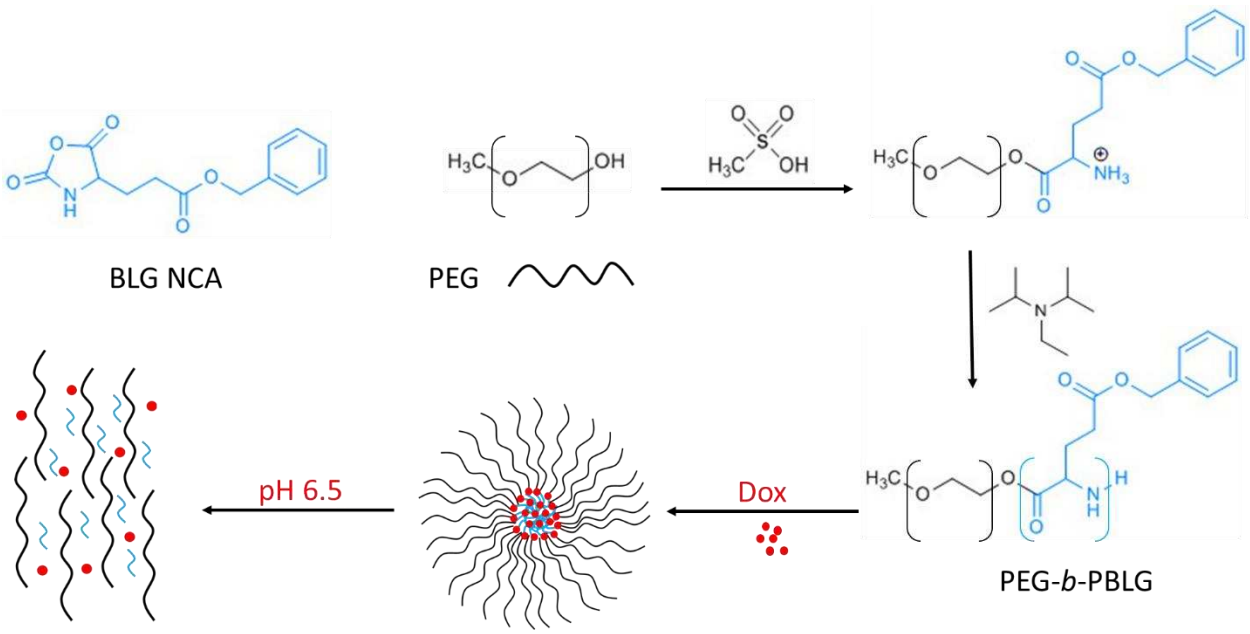

Figure 1. i) Dox release from $PBLG_2$-*b*-PEG_{113} nanoparticles in pH 6.5 and pH 7.4 environments. ii) Dox release from $PBLG_{26}$-*b*-PEG_{113} nanoparticles in pH 6.5 and pH 7.4 environments

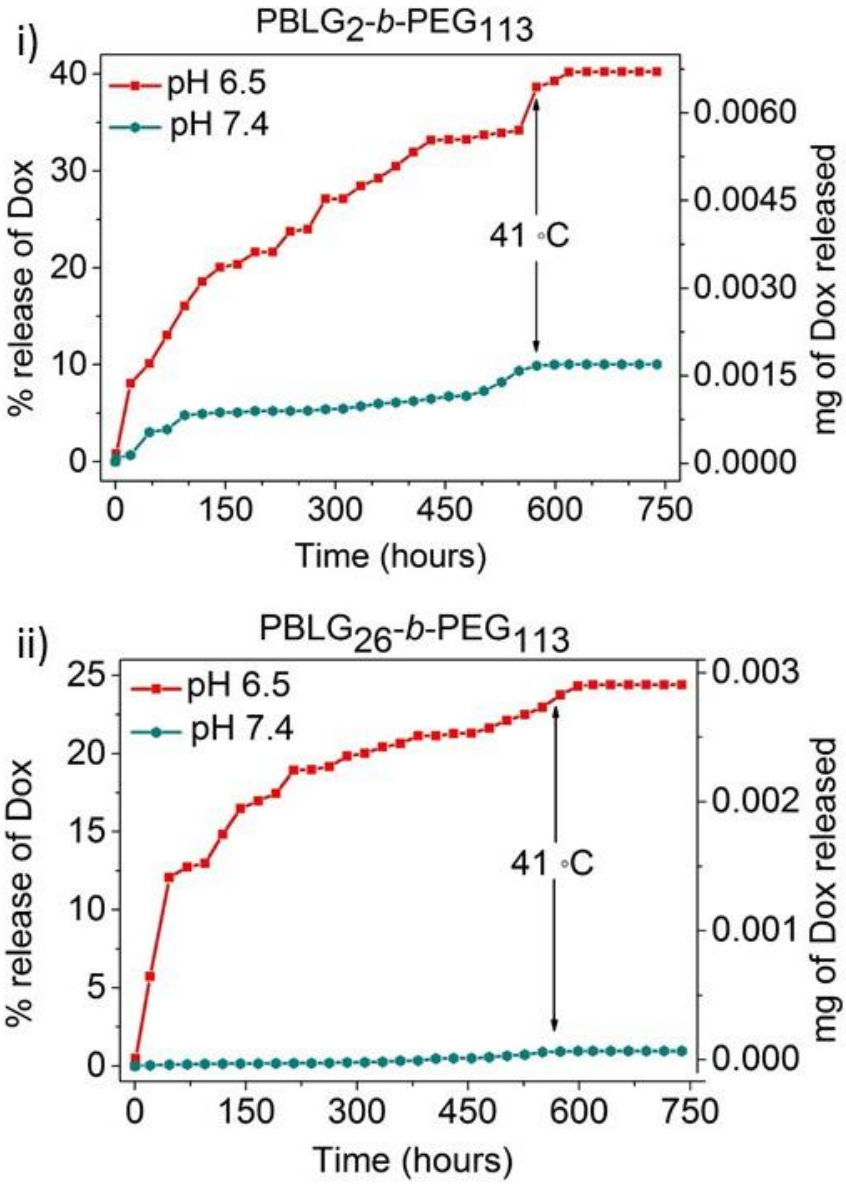

Figure 2. Cytotoxicity of $PBLG_{26}$-*b*-PEG_{113} nanoparticles either empty (NPs) or loaded with Dox (Dox-Loaded NPs), and free Dox on three breast cancer cell lines. Serial dilutions of polymer or Dox-loaded polymer were incubated with i) MCF-7, ii) MDA-MB-231 (triple negative) and iii) MDA-MB-453 (double negative) cell lines.

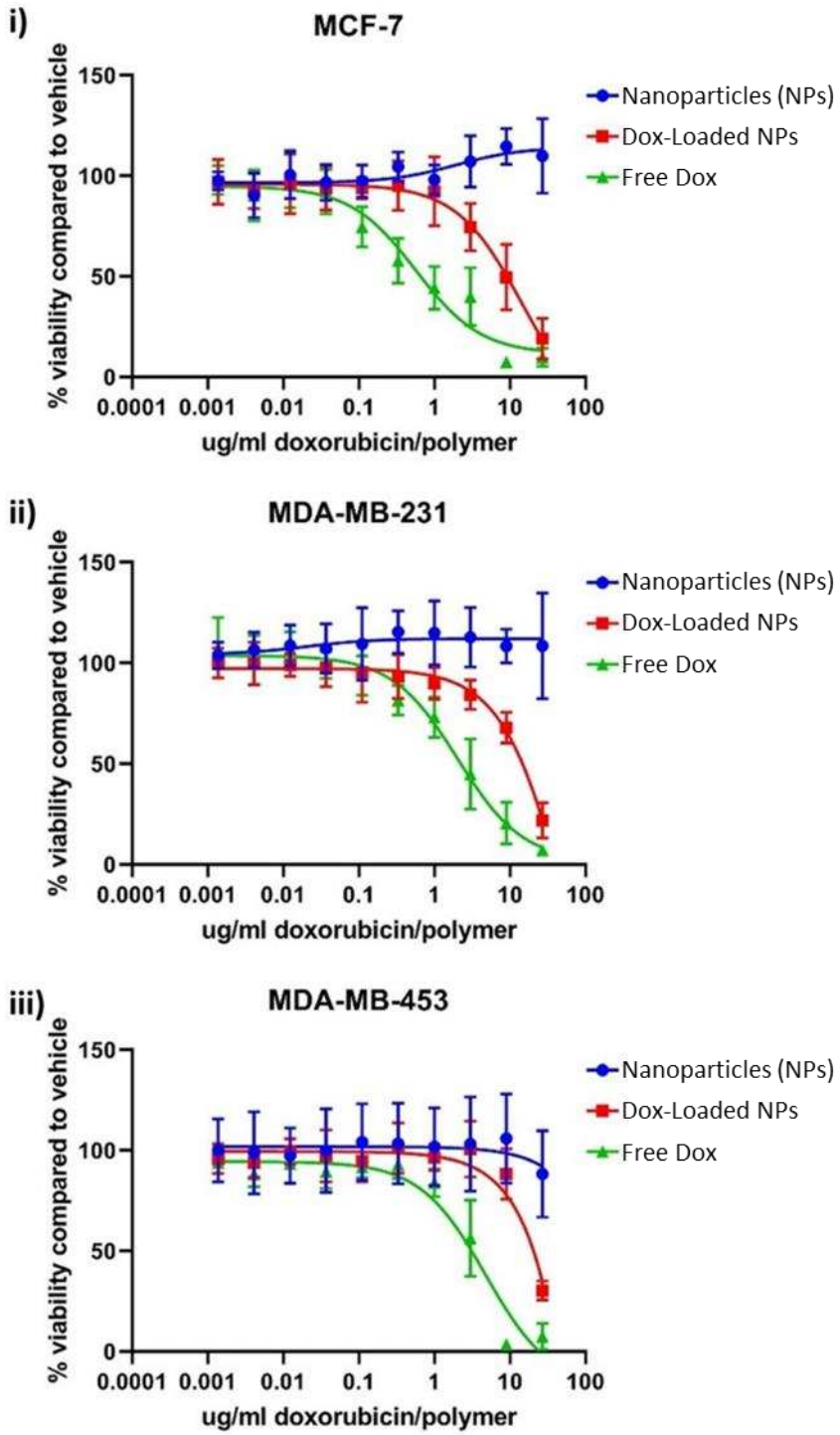

Figure 3. Comparison of free Dox and Dox-loaded PBLG$_{26}$-*b*-PEG$_{113}$ nanoparticles in PHPMA$_{200}$ in PBS buffer solution. Both gels contain an equal mass of Dox; Free dox loading = 0.063 mg of free Dox, and 0.46 mL of Dox-containing PBLG$_{26}$-*b*-PEG$_{113}$ nanoparticles in DMSO, with 43.9% loading efficiency, contain 0.063 mg of Dox. Details of this calculation are provided in the supporting information.

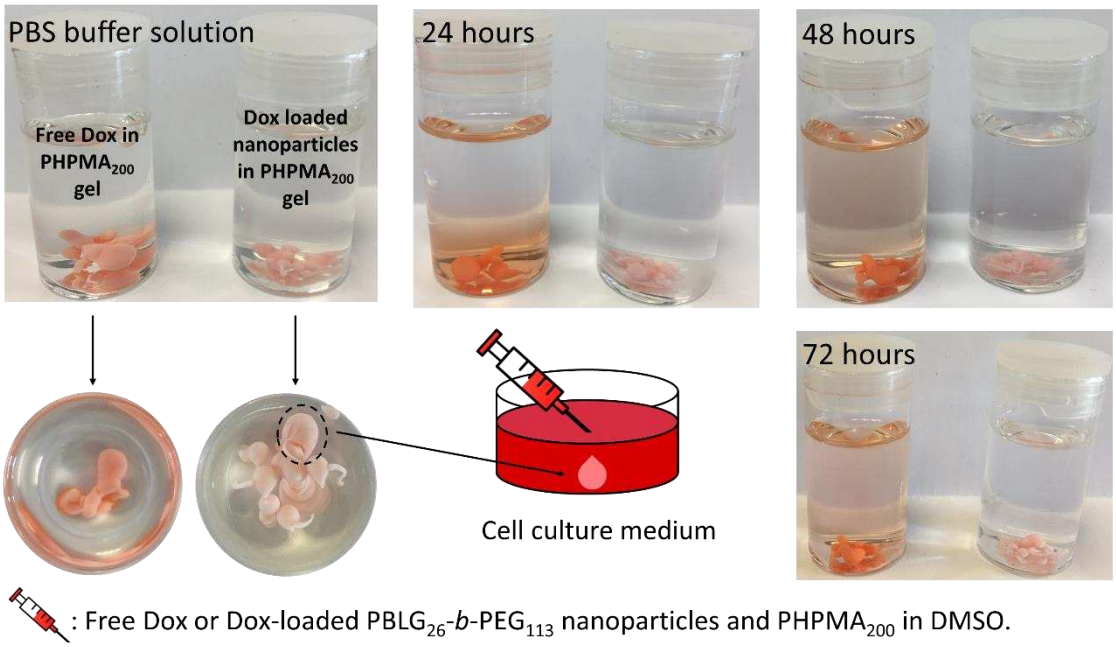

Figure 4. Cell viability studies for the *in situ* formation of PHPMA gel, PHPMA with blank $PBLG_{26}$-*b*-PEG_{113} nanoparticles incorporated, and PHPMA with Dox-loaded $PBLG_{26}$-*b*-PEG_{113} nanoparticles incorporated against i) MDA-MB-231 triple-negative breast cancer cells and ii) HFFF2 fibroblast cells.

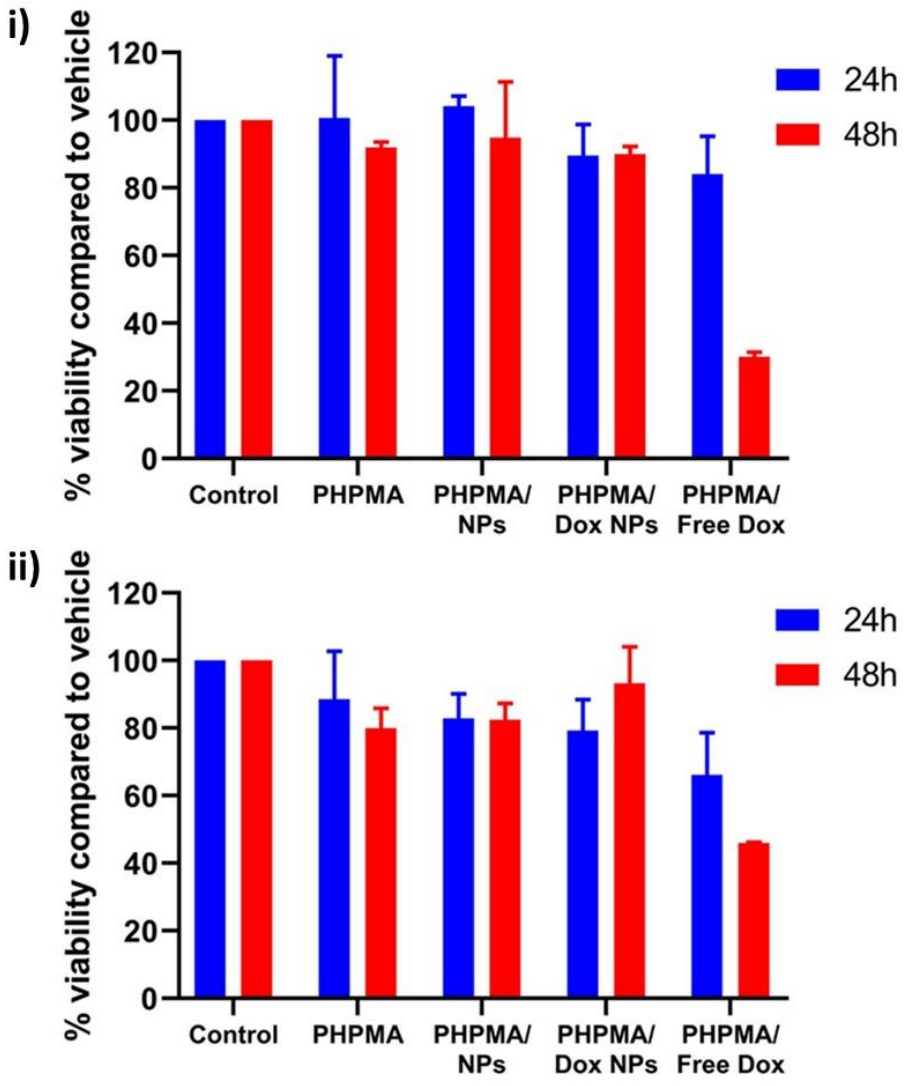

Figure 5. Dox release from PBLG$_{26}$-*b*-PEG$_{113}$ nanoparticles embedded within PHPMA$_{200}$ depot formed in pH 6.5 acetate buffer solution and pH 7.4 PBS buffer solution, at room temperature and at 37 °C.

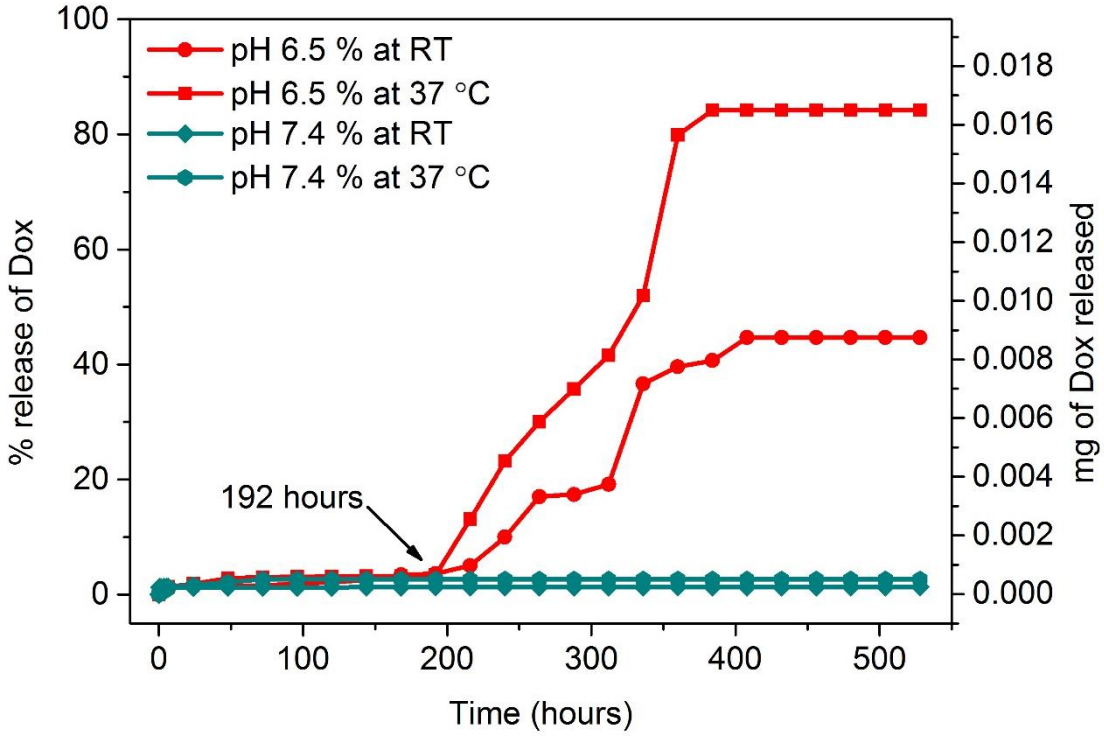

Keywords:

Drug delivery; pH-responsive polymers; thermoresponsive polymers; injectable gels; poly(amino acids); RAFT polymerisation.

*Huayang Yu, Jason V. Rowley, Nicola Ingram, David C. Green and Paul D. Thornton**

Title: Meticulous Doxorubicin Release from pH-responsive Nanoparticles Entrapped within an Injectable Thermoresponsive Depot.

ToC figure:

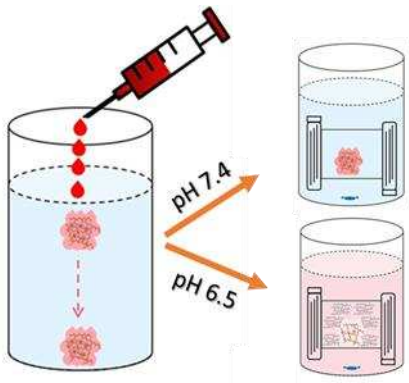

ToC text:

The acid-mediated, temperature-controlled, release of doxorubicin from poly(amino acid) particles embedded within a gel depot is reported. The particles are stable within aqueous solution, and able to withhold an anti-cancer therapeutic for prolonged periods in solution of physiological pH. This injectable system enables localised and controlled chemotherapeutic release to a mildly acidic environment, such as cancer tumour tissue.